J. Fluid Mech. (1980), *vol.* 96, *part* 3, *pp.* 447–460
Printed in Great Britain

On the visual growth of a turbulent mixing layer

By J. JIMENEZ
IBM Scientific Center, Castellana 4, Madrid 1, Spain

(Received 27 November 1978)

Two models are discussed to account for the motion of the concentration interface in turbulent mixing layers. In the first one the interface is treated as a vortex sheet and its roll-up is studied. It is argued that this situation represents only the first stages of layer growth and another model is studied in detail in which a row of vortex cores entrains an essentially passive concentration interface with no vorticity. Both models give values of the spreading rate in approximate agreement with observations, and their relation is discussed.

1. Introduction

The observations of Brown & Roshko (1974) on the plane shear layer provide us not only with a demonstration of the existance of coherent structures in turbulent flows but with an important insight in the mechanism of mixing. Mixing in this context is the process by which two streams are brought in close contact as a preliminary step to molecular diffusion, and this contact is concentrated in the interface between the two fluids. This interface is created as the streams leave the splitter plate and is initially the seat of both velocity and concentration discontinuities. In the first aspect it behaves like an active vortex sheet determining the flow field and being convected by it and, since vortex sheets are known to roll into spiral structures when perturbed, its motion has been proposed as a model for the large structures in the shear layer (Damms & Küchemann 1972). As in most nonlinear problems the calculations involved in this one are diffcult and most of the available information comes from numerical results. It is clear that this process should be important in the first stages of shear layer development since a vortex sheet is clearly present in that zone, but this is not necessarily so in other parts of the layer. This problem is treated briefly in § 2.

Other models have been proposed in which the vorticity in the layer is concentrated in discrete cores (Winant & Browand 1974), and in these models the interface seen in shadowgraphs is not considered as an active sheet but just as a passive concentration discontinuity. The motion of this discontinuity is a much simpler linear problem that can be analyzed quite completely; this is the subject of most of the rest of the paper. It is found that the spiral structures induced in the interface to not grow linearly with time and that an amalgamation mechanism must be postulated if the growth of the layer is not to be stopped completely after a while. Such amalgamations have, of course, been observed in many experiments.

The models considered in this paper are mostly deterministic ones of time-like evolution. However, in order to compute the expected frequency of pairing we must include some considerations of space dependent growth. The last section in dedicated in large part to a discussion of the differences that can be expected between both cases.

0022–1120/80/4368–8140 $02.00

2. The vortex sheet model

Consider an infinite uniform vortex sheet with strength ΔU. If we perturb it locally so that it begins to roll at one point, this roll-up will continue until the sheet develops into a tight spiral whose evolution and growth rate can be easily estimated. We are interested mostly, in the behaviour of the part of the sheet that is about to be engulfed into the central spiral core and whose position determines the growth rate. The motion of this sheet is influenced mainly by the velocity field created by the roughly axisymmetric vorticity concentration in the central core. If we denote this vorticity by $\Gamma(t)$ and use complex co-ordinates centred on the spiral, the trajectory of a fluid particle is governed by

$$d\bar{z}/dt = i\Gamma/2\pi z, \tag{1}$$

where the bar over a symbol stands for complex conjugation. Applying this equation to a particle initially located at a point η on the real axis, its position at time t will be

$$z = \eta \exp\left(-i\int_0^t \Gamma dt/2\pi\eta^2\right). \tag{2}$$

This defines a double-armed spiral with a tight, almost circular, central core and is thus consistent with our assumptions; its size can be characterized by the radius R at the point where the phase is equal to $-\frac{1}{2}\pi$,

$$R^2 = \eta^2(-\tfrac{1}{2}\pi) = \pi^{-2}\int_0^t \Gamma dt. \tag{3}$$

Since the vorticity contained between two particles in the sheet is not changed by the rolling process and the vorticity per unit length is initially ΔU it is clear that the total vorticity contained in the segment of sheet bounded by η and $-\eta$ is just $2\eta\Delta U$; if we consider the core to extend up to $\eta = R$, we can write

$$\Gamma = 2R\Delta U. \tag{4}$$

When this value is introduced into (3) the equation can be integrated to give

$$R = \pi^{-2}\Delta U t. \tag{5}$$

If we now visualize the shear layer as built of structures of this kind which are convected downstream while they grow linearly according to equation (5), the visual growth rate of the layer can be deduced as

$$\frac{\delta}{x} = \frac{4R}{(U_1+U_2)t} = 4\pi^{-2}\frac{\Delta U}{U_1+U_2}. \tag{6}$$

Not only does the velocity dependence of this formula agree with the experimental results (Brown & Roshko 1974) but the numerical value of the coefficient is not far from the commonly accepted one of 0·38.

Actually the problem of vortex sheet roll-up can be treated more rigorously. Considering again an initially undisturbed uniform sheet parametrized by the initial position η, the equations of motion can be written as (Birkhoff 1962)

$$\frac{\partial\bar{z}}{\partial t} = \frac{i\Delta U}{2\pi}\oint\frac{d\eta'}{z(\eta)-z(\eta')}, \tag{7}$$

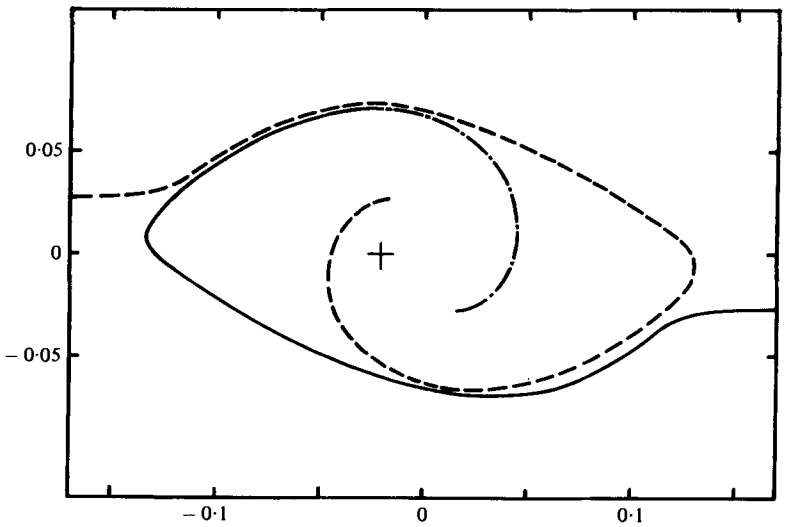

FIGURE 1. A numerical solution to the similarity equation (9) for the roll-up of a uniform vortex sheet.

where the integral on the right-hand side contains the effect of the vorticity distributed along the sheet. This equation admits a similarity solution

$$z(\eta, t) = t\Delta U f(\eta/t\Delta U) \tag{8}$$

which grows linearly in time. The resulting similarity equation,

$$\bar{f} - \xi \frac{\mathrm{d}\bar{f}}{d\xi} = \frac{i}{2\pi} \oint \frac{d\xi'}{f(\xi) - f(\xi')}, \tag{9}$$

is complicated and must be solved numerically. An approximate solution, showing the outer part of the spiral, is given in figure 1 (Jimenez 1977).

Several things can be deduced from this solution. In the first place the growth rate implied is

$$\delta/x = 0{\cdot}28\Delta U/(U_1 + U_2), \tag{10}$$

which is somewhat low but of the right order of magnitude. Second the structure is elliptical with a semi-axis ratio of 1·76; vortices in real layers also seem to be elliptical, and, although there are no reliable measurements of their shapes, an estimate of the elongation can be found from the ratio between vortex spacing and visual layer thickness. In the Brown & Roshko layer this ratio is 1·6 which is close to the figure given above.

Unfortunately no realistic model is possible in which the vortices grow without interaction. In fact, since all structures are convected downstream with the same velocity and do not drift apart it is impossible for them to grow indefinitely without running into each other. When two of them meet the portion of vortex sheet that falls in between is stretched as the two vortices try to roll it into their core until, eventually, either the vortices pair or they drift apart as one of them is captured in another amalgamation. In the last case the intermediate sheet is left as an impoverished interface separating the fluids in the two streams but containing very little vorticity.

The final result of this process is a model in which the vorticity is concentrated in

localized lumps and the two streams are separated by a passive interface which carries a concentration difference but not a velocity jump. This interface is entrained and rolled up by the active cores and constitutes the visual mixing layer observed in the Brown & Roshko shadowgraphs. This interpretation is supported by the pictures of transition taken by smoke or dye injection at the splitter plate (Freymuth 1966; Winant & Browand 1974). Since the dye labels the fluid particles of the vortex sheet formed as the flow leaves the plate, it can be used to follow the evolution of the vorticity contained in these particles; it is easy to see, on inspection of the pictures, that the dye is rapidly concentrated in cylindrical lumps while large parts of the interface are completely depleted. Also measurements by Winant & Browand show definite peaks in the vorticity distribution.

Seen in this light the problem with models, like the one presented above, which depend on the rolling of an uniform vortex sheet is not how well they approximate real shear layers, but why they approximate them at all. We will return later to this point.

3. The entrainment by a row of vortices

Following the reasoning in the previous section we will now try to approximate the shear layer by a periodic linear array of point vortices with wavelength λ and strength $\Gamma = \lambda \Delta U$. these vortices determine a flow field that transports with him a passive interface laying initially along the real axis and separating two individually labelled but otherwise identical fluids. The motion of a point in this interface is given by (Lamb 1945, § 156)

$$\mathrm{d}\bar{Z}/dT = i \cot Z, \tag{11}$$

where

$$Z = X + iY = \pi z/\lambda, \quad T = \pi \Delta U t/2\lambda, \tag{12}$$

are suitable non-dimensional co-ordinates. This complex velocity derives from a potential

$$\Phi = \phi + i\psi = i \ln (\sin Z), \tag{13}$$

in terms of which the equations of motion can be written as

$$d\psi/dT = 0 \tag{14}$$

and

$$d\phi/dT = |d\Phi/dZ|^2. \tag{15}$$

Equation (14) gives the shape of the streamlines and is integrated immediately to

$$\sin^2 X + \sinh^2 Y = k^2 = e^{2\psi}, \tag{16}$$

which can be used to express X, and later the right-hand side of (15), as functions of ϕ and k. Equation (15) can then be integrated to

$$\int_0^{\phi} \left(1 + \frac{4k^2 \sin^2 \phi}{(1-k^2)^2}\right)^{-\frac{1}{2}} d\phi = \frac{k^2-1}{k^2} T, \tag{17}$$

which is easily expressed in terms of the Jacobian elliptic functions and gives finally

$$\sin^2 X = \frac{1+k^2}{2} - \frac{1-k^2}{2} nd\left(\frac{1+k^2}{k^2} T | m\right), \quad m = 4k^2/(1+k^2)^2. \tag{18}$$

These equations describe completely the motion of particles lying initially on the real axis with $X = \arcsin k$. The particles follow closed orbits which for those near a

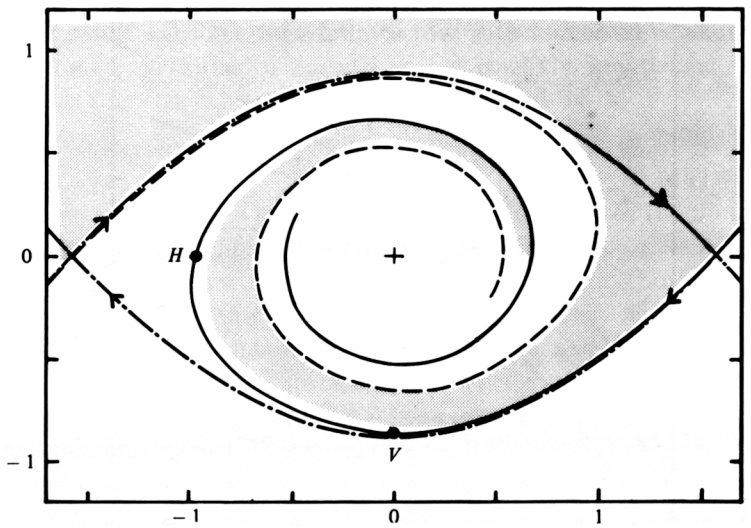

FIGURE 2. Position of the passive interface after being entrained by one of the vortices in a vortex row. ——, – – –, interface; –·–, limiting streamlines. $T = 2{\cdot}5$.

vortex are almost circular and with a short period but which, for those coming from the neighbourhood of one of the stagnation points, approach the limiting streamlines of the familiar 'cat-eye' pattern of the flow, with a period that tends to infinity. As a result a material line lying initially along the real axis is progressively wound into a spiral whose size increases with time as the particles lying closer to the stagnation points, and thus describing wider orbits, are drawn further along the motion. The shape of this line at any given time can be computed from equations (16) and (18), and an example is given in figure 2.

It should be emphasized that while the flow field produced by the row of vortices is stationary the shape of the interface is not, since as time passes the interface is rolled by the central vortex in much the same way as a rubber band would be. In the process it is stretched but not weakened because the property labelling it is a concentration jump that cannot be changed by the flow. In fact it can be considered that new interface is constantly being created near the stagnation points by the two streams of different composition being entrained by the incoming part of the flow in that region (see figure 2). The net effect is that the two fluids are progressively folded into one another and that the spiral roll grows with time. It is precisely this effect that we propose as a model for the visual growth of the layer since the structures seen on shadowgraphs are produced not by any property of the velocity field but by the concentration discontinuities. Also it is clear that those large-scale motions of the concentration field are important in controlling the mixing process.

Obviously only those streamlines that are closed are important in the rollup so that the size of the spiral is limited by the 'cat-eye' streamlines which separate the recirculating regions from the open regions of the flow. The core of the spiral can be represented by an ellipse defined by the points marked as H and V in figure 2 and which can be computed from the equations as

$$X_H = -\arcsin k, \quad T_H = 2k^2K(m)/(1+k^2), \tag{19}$$

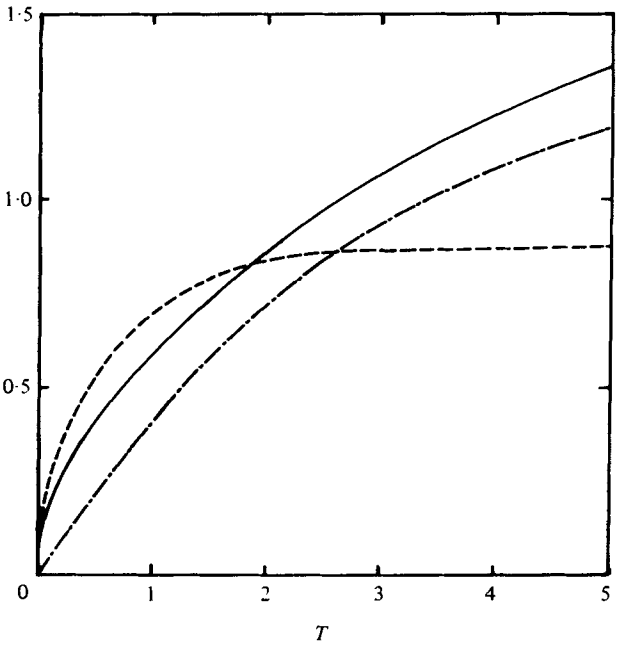

FIGURE 3. Evolution of the non-dimensional parameters of the interface roll-up. – – –, Y_V; ——, X_H; – · –, S.

and $$Y_V = -\operatorname{arcsinh} k, \quad T_V = \tfrac{1}{2}T_H, \tag{20}$$

where K is the complete elliptic integral of the first kind.

These values, together with a representative area

$$S = X_H Y_V,$$

are plotted against ellapsed time in figure 3. At first the spiral is seen to grow like $T^{\frac{1}{2}}$ but later this growth stabilizes and approaches an asymptotic size as the interface begins to fill the space within the limiting streamlines of the 'cat-eye' pattern. Note that the growth of the vertical semi-axis saturates sooner than the horizontal one so that, while at first the structure increases its area and entrains fluid by growing in both directions, soon this entrainment is used only to elongate the horizontal axis. The final shape coincides with that of the limiting streamlines and its elongation is

$$X_H/Y_V = \pi/(2\operatorname{arcsinh} 1) = 1{\cdot}78. \tag{21}$$

4. The effect of pairing

The structures in the previous section do not grow linearly and, after a while, they do not grow at all, so that unless some process is available to rejuvenate old vortices they appear to be a poor model for the entraining structures in the mixing layer. The answer is amalgamation. Vortex pairing is known to be a fast process in which a large amount of entrainment can be considered unlikely, so that the area of the resulting spiral will be close to twice that of the original ones. Meanwhile the wavelength also doubles so that the new limiting streamlines enclose four times as much area and the spiral finds itself with some spare space and resumes its growth.

If we return now to our infinite row of vortices and assume that they all pair at the same time the result will be a new infinite row with longer wavelength. Let the nth pairing, at time t_{pn}, give rise to the nth vortex row; the key parameters will be the fraction of area increase in the amalgamation, defined by

$$\sigma_{i,n+1} = 2(1+\alpha)\,\sigma_{pn}, \tag{22}$$

where σ_i and σ_p are the areas at the beginning and the end of the lifetime of a given structure, and the length θ_n of this lifetime.

To determine this length we have to make assumptions on the pairing mechanism. The observations by Winant & Browand (1974) show vortices rotating around one another for a fraction of a turn before they amalgamate, and they explain this rotation by invoking the well known instability of a vortex row. Observations at higher Reynolds numbers are less clear and have been interpreted at times as the 'tearing' of a vortex core by nearby ones. Moore & Saffman (1975) explain the tearing by showing that a core of finite cross-section is unstable when subject to an external strain above a certain level. In real situations both mechanisms might be difficult to distinguish since they are manifestations of the same basic instability and operate in similar time scales. As vorticity particles are perturbed above or below the dividing streamline they will be moved right or left by the average flow. In strong cores the rotation produced by vorticity is fast enough to take the displaced particle to the opposite stream before the deviation is too large, but in weak cores or point vortices no such mechanism is present and the situation is unstable. The time scale in these cases is the time, $\lambda/\Delta U$, needed by the velocity difference across the layer to span one wave length.

When the nonlinear motion of the most unstable mode of a row of point vortices is computed in detail (see appendix A), the separation of the two vortices involved in a pairing is seen to decrease until it reaches a minimum at the moment in which they cross one above the other, after which they continue to rotate and fly apart again. If we take this moment as the moment of pairing and disregard the question of how the merging of the vorticity actually comes about, we can use as an estimate of pairing period the time needed for the linear instability to carry the point vortices to their crossing amplitude $\frac{1}{2}\lambda$. If we assume an initial perturbation in vortex position with magnitude $\beta\lambda$, this time is (Lamb 1945).

$$\theta = 4\lambda\kappa/\pi\Delta U, \tag{23}$$

where κ is a perturbation parameter constant

$$\kappa = -\ln(2\beta) \tag{24}$$

which measures the amount of initial disorder present in the layer.

If we now remember that in the pairing of two identical vortices the wavelength of the row doubles, the following relations are evident:

$$\lambda_n = \lambda_0 2^n, \quad \theta_n = \frac{4\lambda_0\kappa}{\pi\Delta U}2^n, \quad t_{pn} = \theta_n. \tag{25}$$

Equations (22) and (23) can be written in non-dimensional co-ordinates as

$$S_{i,n+1} = \tfrac{1}{2}(1+\alpha)\,S_{pn}, \quad \Theta = 2\kappa, \tag{26}$$

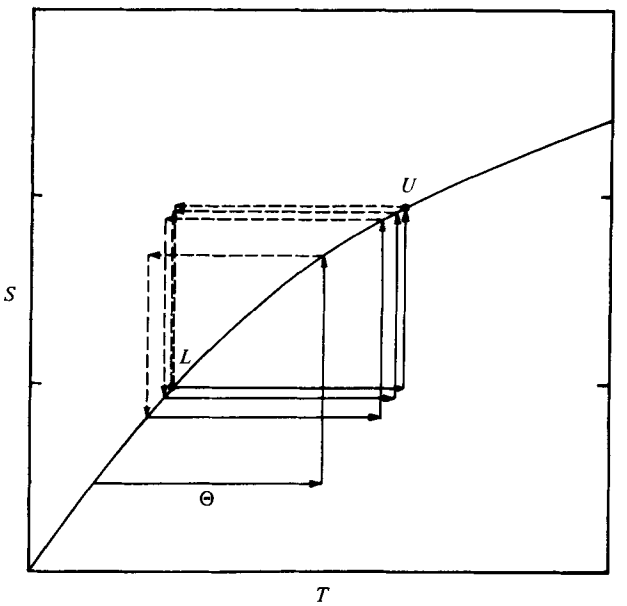

FIGURE 4. The pairing cycle represented on the non-dimensional eddy-growth curve. Solid lines represent growth during lifespan; dashed lines are area changes in pairing. The process approaches a limit cycle with end points L and U.

and, assuming that the pairing of two structures satisfying the S, T relation derived in the last section produces a new structure satisfying that relation the evolution of the process can be followed graphically on the corresponding curve (see figure 4). It is clear from the figure that a limit cycle exists in which

$$S(T_L+\Theta) = \frac{2}{1+\alpha} S(T_L), \tag{27}$$

and it can be shown that the process defined in (26) will always approach this cycle exponentially fast, independently of the initial conditions. The asymptotic state of the mixing layer will be given by this limit cycle and the two important points will be T_L and $T_U = T_L + \Theta$. The maximum spreading rate occurs at T_L and is given by

$$\frac{\delta_L}{x} = \frac{4\lambda_n Y_L}{\pi(U_1+U_2)t_{pn}} = \frac{Y_L}{\kappa}\frac{\Delta U}{U_1+U_2}. \tag{28}$$

The relation between wavelength and visual thickness is also computed easily. Taking as reference the centre point of the nth interval we have

$$\frac{\lambda}{\delta} = \frac{\lambda_n}{1{\cdot}5\delta_{Ln}} = \frac{\pi}{3Y_L}. \tag{29}$$

Both equations are plotted in figure 5 for various values of α and β. The spreading rate is close to the experimental value for perturbation parameters, β, of the order of 5 %. Data for the wavelength vary somewhat for different authors and are usually referred to passing frequencies which do not correspond directly to λ. The accepted values are around 1·5 so that the model predictions are slightly too low.

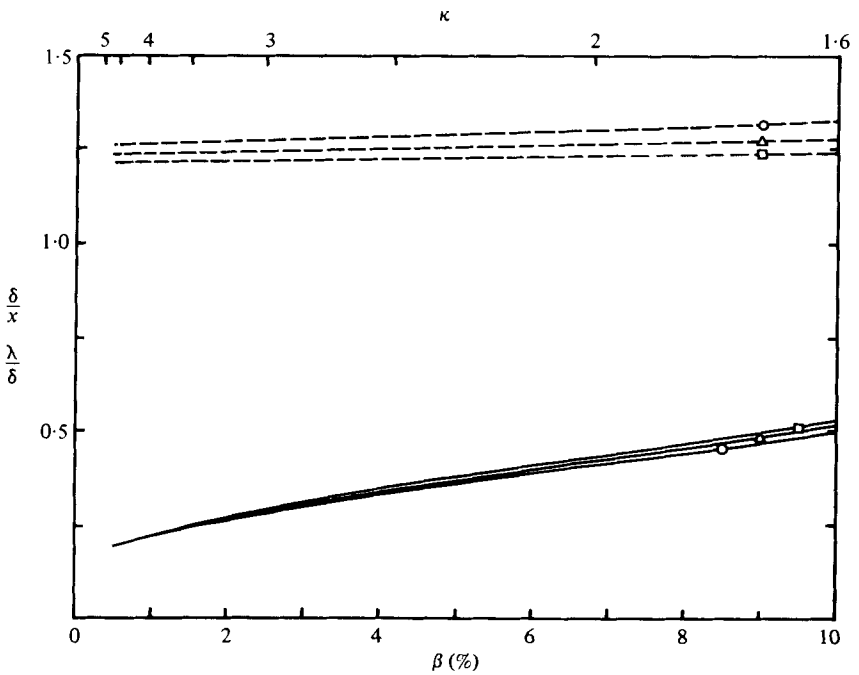

FIGURE 5. Growth rates and wavelengths in the shear layer for different pairings parameters. ——, growth rate; – – –, wavelength. ○, $\alpha = 0$; △, $\alpha = 0{\cdot}1$; □, $\alpha = 0{\cdot}2$.

5. The effect of non-uniformities

The main parameter controlling the properties of the mixing in this model is the initial perturbation level, β, in the layer. This level is presumably related to the amount of free-stream and initial boundary-layer turbulence but the precise relation is not easy to establish. The model predicts that the spreading rate increases with increasing turbulence, which is qualitatively correct, but it also seems to imply that a carefully controlled mixing layer should not spread at all.

In fact the flow inside a mixing layer is turbulent and this turbulence may be able to drive the pairing even under very steady external conditions. However not all the velocity fluctuations in the layer are useful for this purpose. If we consider a vortex row moving by an stationary observer with an uniform velocity he will see strong fluctuations caused by the passage of the vortices, but the velocity induced at the position of the vortex cores will still be zero as long the row is uniform. Vortex rows in real layers are, of course, far from uniform as some vortices downstream have already paired while others are still forming, and the effect of this non-uniformity is indeed able to induce instability.

Assume that two vortices of strength $\lambda\Delta U$ and initially at positions 0 and λ have coallesced into a single one with twice as much vorticity and located at $\lambda/2$. The velocity perturbation induced by this non-uniformity on the position of the kth vortex can be computed by subtracting from the new vortex the effect of the two old ones. The result is a quadrupole

$$u_k = 0; \quad v_k = -\frac{\Delta U}{4\pi} \frac{1}{k(k-1)(k-\frac{1}{2})}. \tag{30}$$

If we now write the equations of motion of the perturbed vortex row as given by Lamb and use the velocities in (30) to drive them we get

$$\frac{dx_j}{td} = \frac{\Delta U}{2\pi\lambda}\Sigma\frac{y_j - y_k}{(j-k)^2}, \quad \frac{dy_j}{dt} = \frac{\Delta U}{2\pi\lambda}\Sigma\frac{x_j - x_k}{(j-k)^2} + v_j, \tag{31}$$

where $x_j + iy_j$ is the deviation of the jth vortex from its equilibrium position. To solve them we define the Fourier transform pair

$$F(p) = \frac{\lambda}{2\pi}\sum_k f_k \exp(-ipk\lambda), \tag{32}$$

$$f_k = \int_0^{2\pi/\lambda} F(p)\exp(ipk\lambda)\,dp. \tag{33}$$

and write (31) as a set of equations among the transforms

$$\frac{dX(p)}{dt} = \mu Y(p), \quad \frac{dY(p)}{dt} = \mu X(p) + V(p), \tag{34}$$

where

$$\mu = \frac{\lambda\Delta U}{4\pi} p\left(\frac{2\pi}{\lambda} - p\right). \tag{35}$$

If we now assume homogeneous initial conditions and keep only terms that diverge with time we can express the solution to (34) as,

$$X(p) \simeq Y(p) \simeq \frac{1}{2}\int_0^t V(p,\tau)\exp[\mu(p)(t-\tau)]\,d\tau, \tag{36}$$

which can be substituted into the inverse transform (33) to recover the motion of the vortices. Since our perturbation velocities and their transforms are independent of time we get

$$x_k \simeq y_k \simeq \int_0^{2\pi/\lambda} V(p)\exp(\mu(p)t + ipk\lambda)\,dp/2\mu(p). \tag{37}$$

The main contribution to this integral comes from the neighbourhood of the most unstable wavenumber, $p = \pi/\lambda$, where $\mu(p)$ is maximum, and expanding the integrand around this point we get the approximation

$$x_k \simeq y_k \simeq (-1)^k\left(\frac{\lambda}{\Delta Ut}\right)^{\frac{1}{2}}\frac{4V(\pi/\lambda)}{\Delta U}\exp(\pi\Delta Ut/4\lambda). \tag{38}$$

From equations (30) and (32) we find the perturbation component $V(\pi/\lambda)$ as

$$V\left(\frac{\pi}{\lambda}\right) = \frac{3\lambda\Delta U}{\pi^2}\sum_{m=1}^{\infty}\frac{1}{(4m^2-1)(16m^2-1)} = 7{\cdot}09\times10^{-3}\lambda\Delta U, \tag{39}$$

which introduced in (38) gives us the evolution of the deviation of the cores from equilibrium. When this deviation is made equal to $\frac{1}{2}\lambda$ we get an equation for vortex lifetime which can be written in terms of the perturbation coefficient κ as

$$e^{\kappa} = 19{\cdot}98\kappa^{\frac{1}{2}}, \tag{40}$$

which is solved to give

$$\kappa = 3{\cdot}64,$$

and, from figures 5 implies a spreading rate

$$\delta/x = 0{\cdot}23\Delta U/(U_1 + U_2). \tag{41}$$

This is to be taken as a lower bound for the visual spreading rate of any mixing layer no matter how steady is the external flow. In deriving it we have had to deviate from our strictly time-like analysis and take into account the spatial development of layer. Other perturbations also derive from this spatial inhomogeneity, the most important one being probably the presence of the splitter plate, and they will add to the effect of pairing to give a higher lower bound to the spreading rate. Other aspects of space versus time growth will be discussed in the next section.

6. Discussion and results

We have presented a simple model of the mixing process in a plane shear layer. As already emphasized in the introduction the model deals mostly with the entrainment of scalar properties like concentration or temperature, which is a linear problem, instead of addressing the much harder problem of nonlinear turbulent diffusion in the flow field. In fact a row of point vortices is a very poor model in this last respect since it induces a mean velocity profile with zero vorticity thickness and an infinite turbulence level. By asssuming a finite size for the vortex cores these problems can be overcome but then a new model has to be found for the growth of the cores. One such model is given by Moore & Saffman (1975) in which they assume that the cores grow by turbulent diffusion and amalgamate by internal instability. Their estimate of λ/δ_ω is in rough agreement with observations and, since it relates to the vorticity distribution, is essentially independent of the arguments in this paper. The pairing mechanism implied is different from the one assumed here but, as noted above, the two processes are approximately equivalent from the point of view of mixing.

Experiments show that the vorticity thickness in the shear layer is about half the visual one suggesting that the vortex cores, if they exist, are smaller than the mixing structures. If this is so the effect of the finite size should not be too important for the entrainment mechanism in § 3, since a more or less circular blob of vorticity looks like a point vortex when seen from outside. In fact the difference in the velocity far field of two vorticity distributions which share total strength and centre of mass is a quadrupole, behaving like r^{-3}, which can be neglected in most cases. This explains why models like the one in § 2 in which vorticity is assumed to be initially distributed in an uniform sheet agree roughly with those in which the layer is modelled as a row of point vortices. In fact a vortex row can be thought of as a vortex sheet plus a row of quadrupoles that is being entrained by the amalgamations into the core chosen as origin. This is also why a uniform row can be used as a useful model for real flows in which there are such things as a splitter plate and vortices at many different stages of pairing. All these events behave like quadrupoles and can be neglected at long ranges, although not in those cases, like pairings, in which close interactions are involved or in those, like instabilities, which are zero in a uniform row.

One result that merits discussion is the relation between vortex lifespan and its time of birth, which can be computed from equations (25) as

$$\theta_n/t_{pn} = 1. \tag{42}$$

This quantity was measured by Roshko (1976) as 0·43 on a mixing layer with a 7:1 density ratio, which is a factor of two too low. More recent measurements by Hernan & Jimenez (1979) on a homogeneous layer give a value of 0·89. The discrepancy is

particularly disturbing since (42) can be derived by simple arguments involving few assumptions.

Consider a vortex that develops in a layer and passes through successive generations separated by pairings. From dimensional considerations we can assume that its lifetime has a probability distribution which is only a function of the ratio θ/t_{pn}, and, since the times of two successive pairings are related by

$$t_{p,n+1} = t_{pn} + \theta_n = t_{pn}(1 + \theta_n/t_{pn}) \tag{43}$$

we can take averages and get

$$\langle\theta_{n+1}\rangle/\langle\theta_n\rangle = 1 + \langle\theta/t\rangle. \tag{44}$$

Since the vorticity resulting from a pairing is, in the average, twice that of the original vortices, all scales in the flow double and the left-hand side of (44) equals 2, so that $\langle\theta/t\rangle = 1$; the argument should be independent of the density ratio in the layer. To avoid this conclusion one should abandon either the concept of successive pairing generations or the hypothesis that lifetime is proprotional to vortex strength. This is conceivable if vortices of different strengths are present in the layer at the same time, as they are in real situations, especially since layers grow in space instead of time. In this case the lifetime could depend not only on the vortex itself but on its neighbours, and the dependence could be complicated. Moreover the concept of a locally uniform layer evolving in pairing steps might not be meaningful any more. Since local uniformity simplifies considerably the calculations it would be desirable to have more measurements of vortex lifetimes, based on larger populations than the ones referred above, to test whether they agree approximately with (42).

It is also of some interest to compute which fraction of the mixing is due to direct growth of the vortices and which to the pairings. Expressing the amount of mixed fluid by the area of the spiral structures it follows from the analysis in § 4 that the relation between the two processes is $(1-\alpha)/\alpha$. Measurements done in a recent computer study of one of the movies by Brown & Roshko (Hernan & Jimenez 1979) show very clearly the growth of vortex area outside pairings. The value of α implied by these measurements is about 0·15.

Although the numerical agreement of the results of this model with experimental measurements is far from exact it is within reasonable bounds of what should be expected from the approximations involved. Moreover the model explains qualitatively many of the observed features in shear layers and opens the way for more sophisticated treatments. One noteworthy aspect is that it lends a plausible reason for the fact that visual coherent structures are prominent in layers at high Reynolds numbers, since a vorticity lump will entrain a passive but turbulent interface in much the same way as a clean laminar one and the resulting large scale concentration distribution will be very much the same in both cases.

Appendix A

The most unstable mode for a row of point vortices is that in which alternate cores move in opposite directions so that pairs rotate around one another. If the origin of co-ordinates is chosen at the centre of one such pair the motion is antisymmetrical and, if the row wavelength is π, half the vortices move along orbits

$$Z_+ = \zeta(T) + 2k\pi, \tag{A 1}$$

and the other half along $$Z_- = -\zeta(T) + 2k\pi. \tag{A 2}$$

The complex velocity induced by the upper row is

$$w_+ = \tfrac{1}{2}i \cot \tfrac{1}{2}(Z-\zeta), \tag{A 3}$$

with a similar contribution from the lower one. When this velocity is to be evaluated at one of the cores the corresponding principal part of the singularity must be subtracted and therefore the motion of the vortex located at ζ is given by

$$\frac{d\bar{\zeta}}{dT} = \lim_{Z\to\zeta} \tfrac{1}{2}i \left[\cot\frac{Z-\zeta}{2} + \cot\frac{Z+\zeta}{2} - \frac{2}{Z-\zeta}\right] = \tfrac{1}{2}i \cot\zeta. \tag{A 4}$$

This, except for a constant factor, is exactly the same equation (11) presented and solved in § 3.

In this case the initial position of the vortex is a small perturbation of $\zeta = -\frac{1}{2}\pi$,

$$\zeta(0) = -\tfrac{1}{2}\pi + \beta\pi, \tag{A 5}$$

and the evolution in time can be read directly from (18). If β is small the resulting motion does not deviate appreciably from the limiting streamline

$$\sin^2 X + \sinh^2 Y = 1, \tag{A 6}$$

and, by expanding (18) around this orbit, the evolution can be written simply as

$$\cos X = \beta\pi \cosh \tfrac{1}{2}T. \tag{A 7}$$

The perturbation in X increases, as expected, exponentially and the time needed for the vortex to get to the crossing point $X = 0$ is

$$T = -2 \ln(\tfrac{1}{2}\beta\pi), \tag{A 8}$$

which, in dimensional co-ordinates is

$$t = -\frac{4\lambda}{\pi\Delta U} \ln(\tfrac{1}{2}\beta\pi), \tag{A 9}$$

and does not differ significantly from the linear value used in § 4.

Except for this evolution in time all other properties of the orbit can be computed along the approximate trajectory given in (A 6) and expressed as simple functions of X that are valid for all small values of β. The distance, $2|\zeta|$, between vortices and the strain, $e = |dw/dz|$, imposed on the cores by the flow are computed in this way on table 1. It is clear that as the vortices proceed to the crossing point their separation decreases and the pairing system becomes more compact as seen from the outside, but the imposed strain also decreases making it harder for the Moore & Saffman instability to disrupt the cores.

X	$2\|\zeta\|$	e
1·57	3·14	0·33
1·31	2·67	0·33
1·05	2·30	0·32
0·78	2·05	0·30
0·52	1·88	0·25
0·26	1·79	0·19
0	1·76	0·16

TABLE 1

REFERENCES

BIRKHOFF, G. 1962 Helmholtz and Taylor instabilities. *Proc. Symp. in App. Math.* vol. XIII, pp. 55. Providence, R.I.: AMS.

BROWN, G. L. & ROSHKO, A. 1974 On density effects and large structure in turbulent mixing layers. *J. Fluid Mech.* **64**, 775–816.

DAMMS, S. M. & KÜCHEMANN, D. 1972 On a vortex sheet model for the mixing between parallel streams. *Roy. Aircraft Establishment Tech. Rep.* 72139.

FREYMUTH, P. 1966 On transition in a separated laminar boundary layer. *J. Fluid Mech.* **25**, 683–704.

HERNAN, M. A. & JIMENEZ, J. 1979 Automatic analysis of fluid flow pictures. *Proc. 2nd Symp. Turbulent Shear Flows*, London.

JIMENEZ, J. 1977 Numerical simulation of mixing layer vortices. In *Structure and Mechanics of Turbulence*, vol. I (ed. H. Fiedler). *Lectures Notes in Physics*, vol. 75. Springer.

LAMB, H. 1945 *Hydrodynamics*. Dover.

MOORE, D. W. & SAFFMAN, P. G. 1975 The density of organized vortices in a turbulent mixing layer. *J. Fluid Mech.* **69**, 465–473.

ROSHKO, A. 1976 Structure of turbulent shear flows: A new look. *A.I.A.A. Paper*, 76–78.

WINANT, C. D. & BROWAND, F. K. 1974 Vortex pairing: the mechanism of turbulent mixing-layer growth at moderate Reynolds numbers. *J. Fluid Mech.* **63**, 237–255.